A Wear Particle Sensor Using Multiple Inductive Coils Under a Toroidal Magnetic Field

YIN BAI[1], **YONG LIU**[2], **LEILEI YANG**[1], **BIN FAN**[2], **PENG ZHANG**[2],
AND SONG FENG[1], (Member, IEEE)

[1]School of Advanced Manufacturing Engineering, Chongqing University of Posts and Telecommunications, Chongqing 400065, China
[2]State Key Laboratory of Smart Manufacturing for Special Vehicles and Transmission System, Baotou 014030, China

Corresponding author: Bin Fan (binfan@imau.edu.cn)

ABSTRACT Inductive wear particle sensors have been widely studied due to their ability to monitor the wear status of equipment in real time. To detect wear particles more precisely, a wear particle sensor based on multiple inductive coils under a toroidal magnetic field is proposed in this paper. With inductive coils located near a stronger magnetic field, the sensor can not only ensure the flow rate, but also enhance wear particle detection accuracy. The proportional relationship between the signal and the wear particle velocity and the excitation current is discussed in this paper. The crosstalk phenomenon among different inductive coils was also investigated by single particle experiments and lubricating oil dynamic experiments. In the dynamic oil experiment, the sensor detected 13μm particles under a flow rate of 570 mL/min, which satisfied most industrial online monitoring demands.

INDEX TERMS Inductive debris sensor, multiple coils, real-time oil monitoring.

I. INTRODUCTION

Modern industry development has produced more machinery and equipment for addressing repetitive and hazardous tasks. However, while improving efficiency, mechanical equipment can be prone to damage after long-term wear, which may lead to machinery failure or catastrophic accidents. Therefore, condition based maintenance (CBM) and nondestructive evaluation (NDE) have become indispensable to advanced manufacturing engineering. Over the past decades, there has been a growing demand for online wear monitoring, and researchers have studied different condition monitoring methods to provide early fault prediction and operational management for complex mechanical systems [1]–[3], such as vibration detection and oil wear detection. One effective approach to monitoring wear is vibration detection, which can monitor abnormal vibration frequency characteristics. Although vibration detection technology is direct, real-time, and covers many fault types, the signals may not be obvious as shock absorption facilities between the mechanical components may mask them. Furthermore, due to the large amount of data from complex vibration signals, a larger memory is usually required for storage and processing. Therefore, complex signal transmission has made vibration monitoring difficult during the initial wear process and while detecting mechanical internal wear [4], [5]. Considering these factors, it would be better to directly determine the wear state and the wear mode by detecting particles in the machine lubricating oil.

During mechanical equipment normal operations, the particle size generated by friction is generally 10-20 μm. However, with poor load or assembly, abnormal friction often occurs between friction pairs, resulting in particles larger than 50 μm [6], [7]. Different techniques have been adopted to detect wear particles and monitor machine tribological performance. Optical methods can be used to determine the wear particle shape, size, and rate [8]–[11]. Inductive or eddy current methods can be used to determine the granularity and magnetic characteristics of particles, and the capacitive method can detect permittivity differences [12]. Among them, inductive or eddy current sensors are widely used in online detection due to their simple installation, large sensing zones, and low influence from bubbles and water droplets.

Through inductive or eddy current methods, particle movement changes the magnetic field distribution [13]–[16]. To study the coupling relationship between metallic materials

and magnetic fields, Adewale *et al.* analyzed how the electromagnetic characteristics of different materials contributed to eddy currents, which could be used to measure the displacement of weakly magnetic ferrous metal materials and components with low relative permeability [14]. Jia's also modeled wear particles, magnetic fields, and the coupling between adjacent particles. That group found that the magnetic potential generated by two passing particles was larger than that of the two separately superimposed particles, and the distance between the two particles was inversely proportional to the magnetic coupling effect, providing a reference model for electromagnetic coupling [16].

Different structures and more complex sensor models have been proposed to improve detection. Han *et al.* analyzed several inductive sensors and found that symmetrical coil design reduced the noise effect [17]. Therefore, symmetrical magnetic field design and symmetrical multipipe design have gradually become common in inductive methods. By undersampling the signal collected by the parallel inductive coil, the sensor proposed by Li *et al.* was able to detect 75-150 μm wear particles with a 21 ml/min oil flow rate [18]. Later, to improve the sensor sensitivity, they used inductance-capacitance (LC) to ensure that the sensor could detect iron particles larger than 20 μm and copper particles larger than 55 μm [19]. Based on this sensor, Zhu *et al.* proposed a 3×3 wear debris sensor array. Through synchronous sampling and signal processing, the flow rate was increased to 460 ml/min, and particles larger than 50 μm could be detected, which greatly improved performance [20]. However, the large amount of data generated by multiple channels at the same time has become an obstacle to real-time signal processing. The amount of signal data during actual sampling is very large (a 10-channel sensor at a sampling frequency of 100 MHz generates 24.3 T of data in one hour [20]). Therefore, there are additional requirements for real-time signal equipment. In addition, lubricating oil degradation is a complex and complicated process, and it is inadequate to assess its condition by monitoring only small oil samples. To meet mechanical equipment oil sensor requirements, the sensor oil pipe diameter is gradually increasing. Therefore, Yi *et al.* analyzed the ratio S of the sensor detection accuracy to the tube diameter. The smaller S was, the higher the sensitivity of the sensor. They compared the S value of different sensors and designed an inductive sensor with a diameter of 34 mm that detected ferromagnetic particles over 120 μm [21]. These studies have advanced inductive sensors and our understanding of wear particle and inductive coil characteristics.

Although various structural sensors have been studied, most studies only focused on detection accuracy or circulation because modern industry demands that inductive wear particle sensors provide both precise monitoring and high flow. It is worth mentioning that some sensors with large tube diameters do not account for errors caused by magnetic field inhomogeneity and wear particle trajectory. Hence, this paper proposes a multiple inductive coil inductive sensor under a toroidal magnetic field. Each inductive coil was wound on a pipe with an outer diameter of 3 mm and an inner diameter of 1.9 mm. With the inductive coils placed on the edge of the toroidal symmetrical magnetic field, the sensor sensitivity was improved while weakening the influence from the abrasive particle movement trajectory, and the oil flow could be controlled by the number of pipelines. The remainder of this paper is organized as follows: Section II presents the sensor structure and simulation analysis. Section III introduces the experimental devices. The experimental results in Section IV shows that the sensor exhibited relatively high sensitivity without interference from crosstalk signals.

II. SENSOR STRUCTURE AND SIMULATION ANALYSIS
A. SENSOR STRUCTURE DESIGN
The sensor proposed in this paper was composed of three main parts: magnetic circuit, sensor, and housing. An electromagnet structure was formed by the excitation coil and the magnetic poles. The excitation coil was wound on the magnetic pole with 1,000 turns of copper wire with a diameter of 0.5 mm. To improve the sensor sensitivity, an air gap was set between the magnetic poles. When the excitation coils were energized, the electromagnet structure generated a high-intensity magnetic field at the air gap. The sensor adopted a rotationally symmetric structure to generate a gradient annular magnetic field inside the hollow cylindrical magnetic pole. The magnetic field intensity was greatest near the magnetic pole inner wall and decreased in the radial direction with the smallest intensity in the center of the pipe. The cross-sectional view of the excitation coil and magnetic pole is shown in Fig. 1(a).
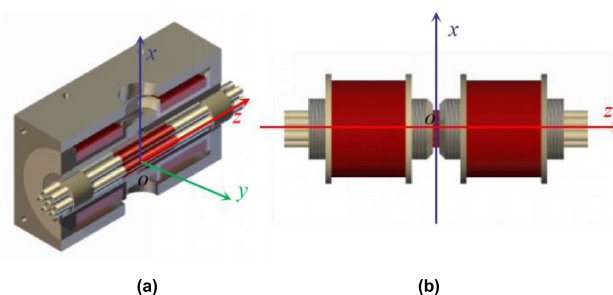

FIGURE 1. Schematic diagram of sensor structure. (a) cross-sectional view. (b) internal front view.

The sensor included multiple inductive coils, and the inductive coil used was wound on a ceramic tube with an outer diameter of 3 mm and an inner diameter of 1.9 mm. Each coil was wound with 2,000 turns of 0.05 mm copper wire with a length of 30 mm. During the experiment, the sensor used six inductive coils in the surrounding position and an inductive inductive coils in the surrounding position and an inductive coil in the middle as a reference coil. The outer inductive coil in the middle as a reference coil. The outer housing shielded external noise and maintained sensor stability.

Although the sensor utilized multiple inductive coils, the working principle of each inductive coil was the same since the inductive coils were in a toroidal magnetic field. We developed a mathematical model for one inductive coil. We established a coordinate system with the sensor air gap center as the origin. The magnitude of the inductive voltage in the magnetic field is related to the change in magnetic flux caused by wear particle movement:

$$u = N \lim \frac{\Delta \varphi}{\Delta t} \tag{1}$$

where u is the inductive voltage, N is the inductive coil turn number, and $\Delta \varphi$ is the magnetic flux change during Δt.

When only a single coil was considered, the sensor model was similar to a previous study [22]. The previous study assumed that the passing wear particles were equivalent to a $\delta_x \times \delta_y \times \delta_z$ cube, and the sensor output could be expressed as:

$$u = N N_D I \delta_x \delta_y \delta_z \frac{\mu(\mu_r - 1)}{\mu_r} \lim_{\Delta t \to 0} \frac{\sin \alpha}{l^2(x) \Delta t}$$

$$= -2 N N_D I \delta_x \delta_y \delta_z \frac{\mu(\mu_r - 1)}{\mu_r} v \cdot \frac{d}{dx} (\frac{\sin \alpha}{l^2(x)}) \tag{2}$$

where N_D is the excitation coil turn number, v is the velocity of the particles along the x-axis, μ_0 is the vacuum permeability coefficient, μ_r is the wear particle permeability coefficient, l_p is the length of the P-th path, and α is the angle between the magnetic field direction and the cuboid xy-plane.

B. MAGNETIC FIELD DISTRIBUTION INSIDE THE SENSOR

The magnetic flux density radial and axial distributions in the sensor under a static magnetic field are presented in Fig. 2. The simulations illustrated that the sensor magnetic field was unevenly distributed. However, the surrounding inductive coils were located in the strongest area of the axial center and in the radial direction where the magnetic field was strong. Moreover, the coil in the radial center was verified as the reference coil in the simulation. The design ensured that the six surrounding inductive coils were at the same position in the magnetic field and avoided signal errors caused by different wear particle positions. In addition, compared to the middle coil, the surrounding coils obtained clear inductive signals, which were conducive to optimizing the detection accuracy.

In the simulation, cubes with side lengths of 0.2 mm, 0.4 mm, 0.6 mm, and 0.8 mm passed through the pipe at a velocity of 2 m/s, and the peak-to-peak values of the particles passing through the middle and surrounding pipes are shown in Fig. 2. When the inductive voltage was small, the signal difference between the middle and surrounding coils was close under the same conditions. However, as any factor increased, such as the inductive voltage amplitude or the size or velocity of wear particles, the surrounding coil signal was significantly better than that of the middle coil. During mechanical operations, the lubricating oil speed passing through the pipeline can increase, and the surrounding coils gradually emerge as an advantage for wear particle detection.
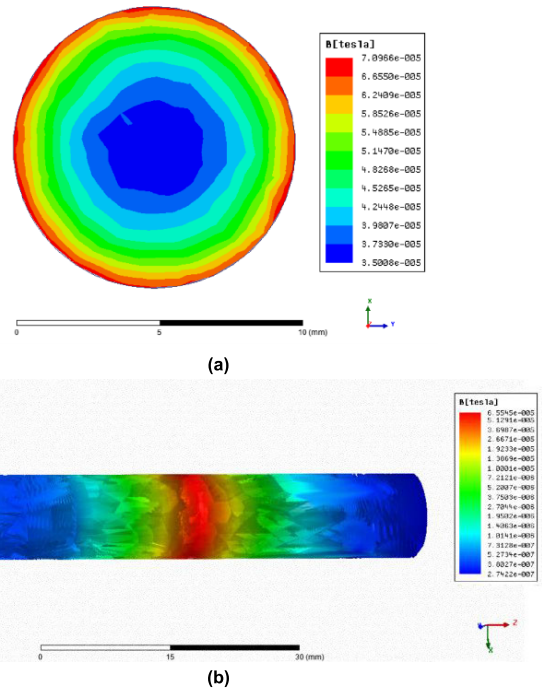

(a)

(b)

FIGURE 2. Schematic diagram of magnetic field distribution. (a)radial direction. (b)axial direction.

C. CROSSTALK BETWEEN INDUCTIVE COILS

When wear particles pass through the inductive coil in a mechanical system, the magnetic flux changes. Therefore, the inductive coil that does not pass through the particles detects the magnetic flux change, and crosstalk signals may be generated near pipes. Crosstalk between different coils was analyzed by simulations to study sensor responses under this condition. For example, when a cube with a side length of 0.8 mm passed through a surrounding pipe (set as surrounding pipe 1) at a speed of 2 m/s, the inductive voltage signal reached 334 μV, and a 1.85 μV crosstalk signal in the opposite direction was generated in the middle or another surrounding inductive coil. However, when the same particle passed through the middle pipe, the generated inductive voltage was only 237 μV at an excitation of 0.5 A, while the detectable inductive voltage of the surrounding pipe was approximately 0.7 μV. Through comparing Fig. 4 and Fig. 5, we noticed that the inductive voltage signal of the particles passing through the surrounding pipe during the simulation was significantly better than that passing through the middle pipe. Due to the weaker intensity of the middle magnetic field, the interference effect was more obvious, which resulted in the middle coil inductive voltage being smaller and not stable enough.

In a magnetic field, the coil flux linkage is equal to the product of the number of coil turns and the average magnetic flux passing through each coil turn. To obtain each coil's flux linkage, cube particles with an edge length of 0.8 mm were modeled as passing through one of the surrounding coils. From Fig. 6, it can be seen that the ferromagnetic
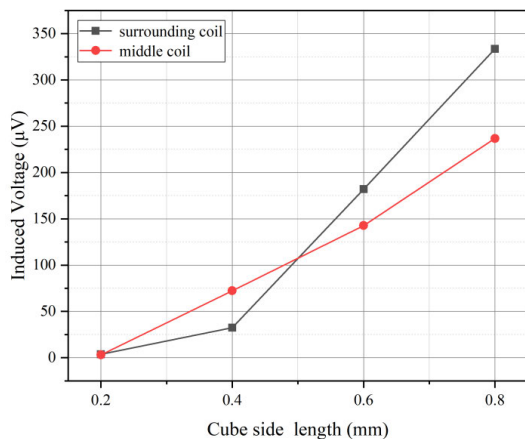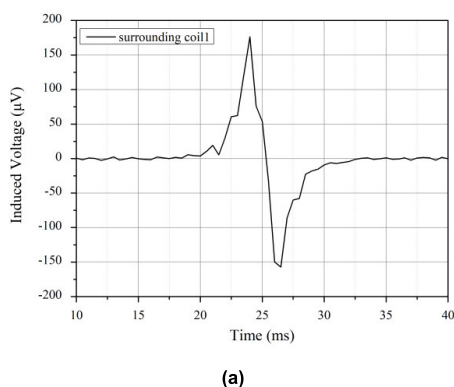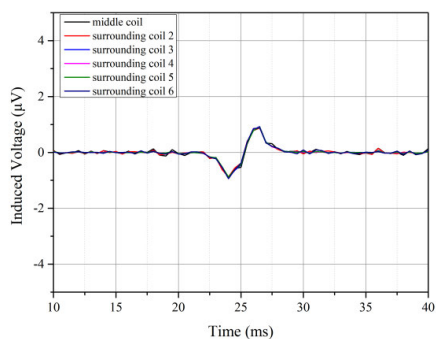
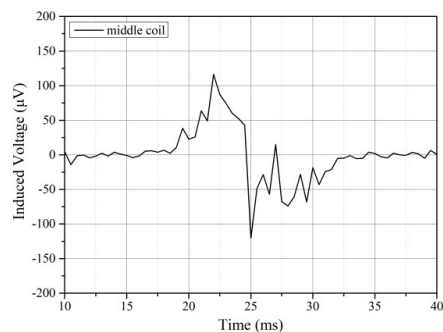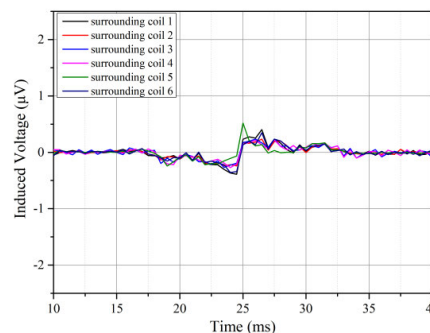**FIGURE 3.** Simulated inductive voltages of different sizes of wear particles.

(a)

(b)

FIGURE 4. Simulated signal when debris passed through the surrounding pipe (the edge length of debris was 0.8 mm). (a)Debris signal. (b) Crosstalk signal.

(a)

(b)

FIGURE 5. Simulated signal when debris passed through the middle pipe (the edge length of debris was 0.8mm). (a)Debris signal. (b) Crosstalk signal.

wear particle will enhance the nearby original magnetic field when it passes, and therefore contribute to the growth of the flux linkage of the inductive coil of the pipe where the particle is located. The flux linkage of the inductive coils of other pipes will be reduced due to the magnetization of ferromagnetic wear particle, which is shown in Fig. 4 and Fig. 5. Furthermore, since the magnetic field of the middle coil was weaker, its flux linkage is always smaller than that of the surrounding coils. Simulation analysis indicated that the particle signal of one inductive coil contributed to crosstalk from opposite waveforms in other inductive coils.

III. EXPERIMENTAL DEVICE

A. SINGLE PARTICLE EXPERIMENTAL DEVICE

The single particle experimental device was used to detect the influence of different factors on the output voltage signal. According to the mathematical model in Part II, the wear particle signal had a linear relationship with the particle velocity and the excitation current. The particle size used in this single particle experiment is shown in Fig. 7. To verify sensor performance and the influence of different pipe arrangements on the output signal, nylon rope was utilized to control the speed of the particle passing throughthe pipe. The UNIT-3305 DC power supply drove constant, direct current through the excitation. For accurate velocity control, a stepping motor controlled the particles on the nylon rope to cycle through the tubing multiple times. To improve the signal level, a low-noise differential amplifier was adopted with gain G=500. We used the average value of 10 sets of data collected under the same conditions. The experimental results are analyzed and discussed in Chapter IV.

B. LUBRICANT OIL DYNAMIC EXPERIMENTAL DEVICE

Wear particle generation and movement in lubricating oil is a random process, and wear particle trajectories are complicated. To simulate wear particles passing through the oil circuit, a stirrer uniformly lubricate oil with different wear particle contents. The experimental lubricant oil sample was
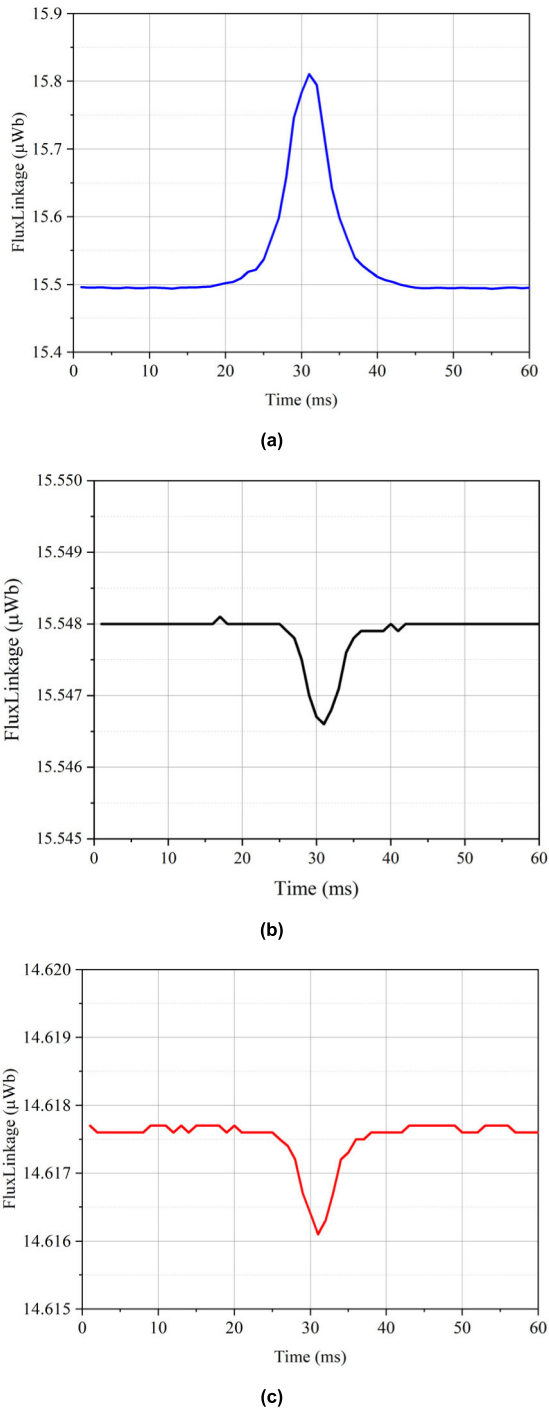
(a)

(b)

(c)

FIGURE 6. The flux linkage of different coils changed when the particle passed through the surrounding coil. (a) Surrounding coil. (b) Another surrounding coil. (c) Middle coil.

passed through the sensor at a constant flow rate by a peristaltic pump. In actual working conditions, due to the small sensor diameter, the sensor could not be directly connected to the oil circuit, but rather to the bypass for wear particle monitoring. As shown in Fig. 8, when the particles passed through the sensor, inductive signals were generated. Thus, the amplified signal could be collected by an acquisition
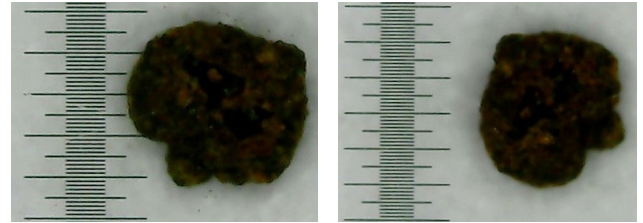

FIGURE 7. Experimental particle (1DIV=10μm).

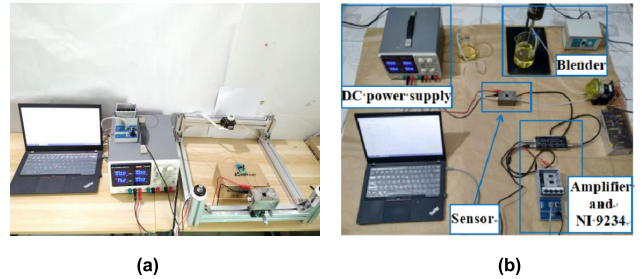(a)   (b)

FIGURE 8. Experimental device. (a) Single particle experimental device. (b) Lubricant Oil dynamic experimental device.

card (NI-9239) for data analysis and mechanical condition diagnosis.

IV. EXPERIMENTAL RESULTS AND DISCUSSION
A. CROSSTALK BETWEEN INDUCTIVE COILS
Since the inner diameter of the magnetic poles was 12 mm, after placing seven inductive coils with an outer diameter of 3 mm inside, there was a small gap between each inductive coil. Therefore, single particle experiments were implemented to analyze the occurrence of crosstalk phenomenon, which was verified in the simulation. Fig. 9 shows the inductive voltage generated by different coils when a particle passed through the sensor at 1.41m/s under an excitation current of 0.5A. In the experiment, when the particle passed through a surrounding pipe, there was no effect between other surrounding pipes, but crosstalk occurred between the surrounding pipe and the middle pipe. This could be explained as when particles cut the induction magnetic lines through the surrounding coils, part of the induction magnetic lines also passed through the middle coil. Therefore, the middle coil also produced more obvious changes than the surrounding coils, and this kind of crosstalk between adjacent surrounding coils was easily masked by noise.

B. EFFECT ON CURRENT AND PARTICLE VELOCITY
The velocity of the wear particles and the intensity of the magnetic field directly cause a difference in the amount of magnetic flux change, which affects the sensor output signal. To verify the influence of the sensor output on the current and velocity, the experiment analyzed the output voltage when a fixed ferromagnetic particle passed through different pipelines. As shown in Fig. 10 and Fig. 11, the inductive voltage had an approximately linear relationship with the particle velocity and excitation current. We also note that with a larger current and stronger magnetic field strength,
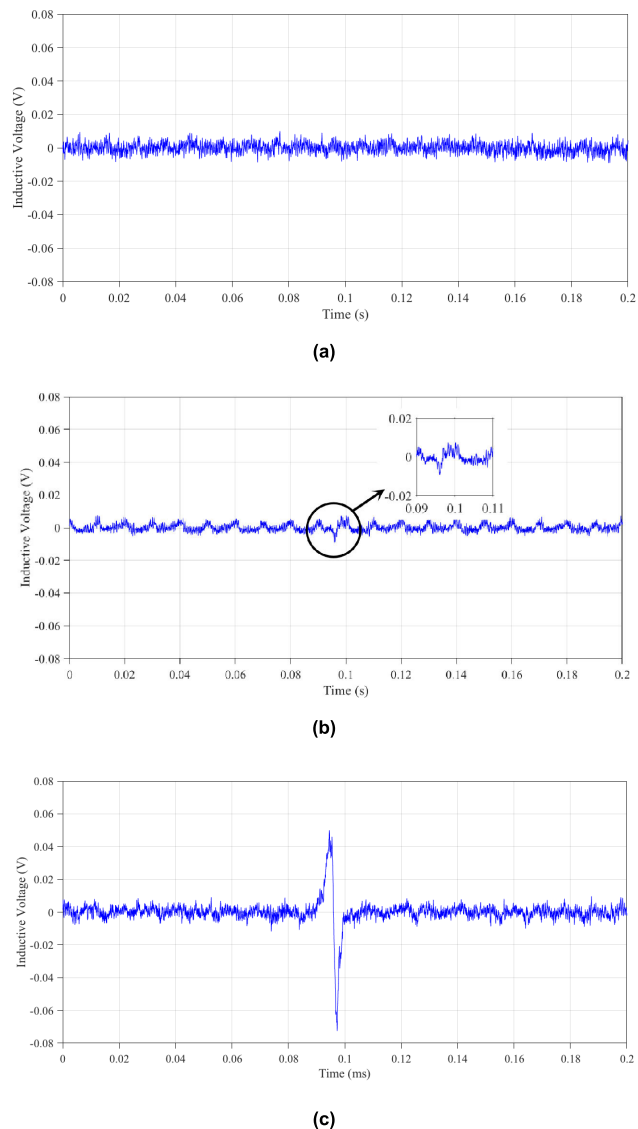
(a)

(b)

(c)

FIGURE 9. Signals of different coils (when a particle passes through a surrounding pipe). (a) Another surrounding coil. (b) Middle coil. (c) The coil where the particle is located.

the corresponding voltage growth rate was faster. Moreover, due to the magnetic field strength attenuation in the radial direction, the middle coil voltage linearity was better than that of the surrounding coil. The magnetic field intensity near the magnetic pole was stronger, which led to a better sensor output signal. Since the inductive voltage in the experiment was obtained by taking the average of 10 sets of experimental data, we calculated the standard deviation of each data point to further discover the degree of experimental data dispersion and error. As shown in Fig. 10 and Fig. 11, the standard deviation of each data point during the experiment was maintained at approximately 0.005, which proved high experimental stability and repeatability.

C. EFFECT ON PARTICLE SIZE

To further analyze the relationship between the inductive voltage and the particle size, results are shown in Fig. 12,
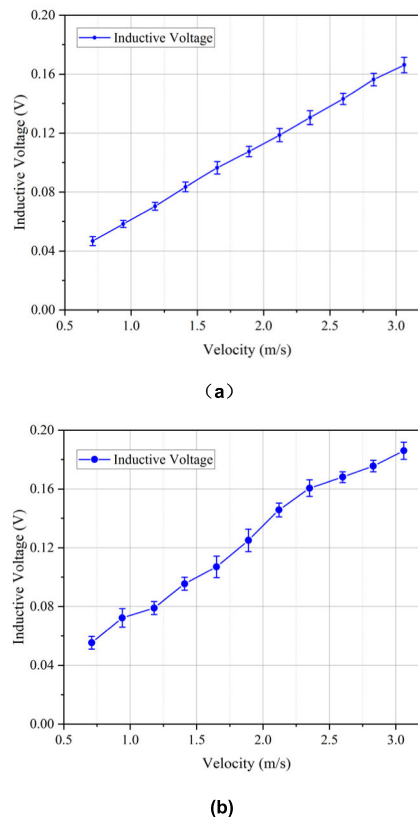

（a）

(b)

FIGURE 10. Inductive voltages at different speeds. (a) Middle coil. (b) Surrounding coil.

where the x-axis represents the volume of wear particles and the y-axis represents the inductive voltage after amplification. The experiment induced wear particle diameters of 0.5 mm, 0.7 mm, and 0.9 mm. As shown in Fig. 12, the inductive voltage had a linear relationship with the wear particle volume, and as the speed increased, the inductive voltage also clearly increased. The experimental results were consistent with the formulas in Section II and the data in Part C, which was beneficial to estimating the wear particle size.

In addition, different experiments were performed on oil samples with different concentrations, and the inductive signals are shown in Fig. 13. The experimental results more intuitively show the signal distribution of the sensor in actual oil monitoring. With the same concentration, the oil sample with larger particles showed less signal and higher peak value.Under the same particle size, the higher the concentration, the greater the number of signal pulses detected. However, due to the different particle paths and the inhomogeneous magnetic field distribution inside the sensor, the signal peak had a certain randomness.

D. DETECTION SENSITIVITY IN A DYNAMIC OIL EXPERIMENT

We verified that the sensor obtained an effective signal when a single wear particle passed through, and the obtained signal met expectations. To confirm the sensor's capability for measuring oil properties in dynamic conditions with multiple
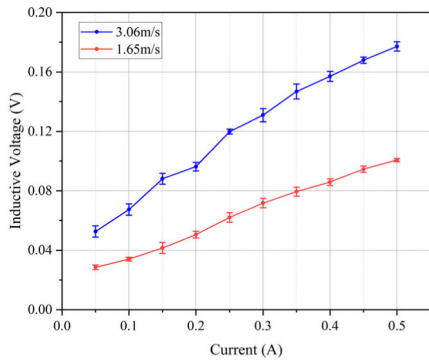
(a)
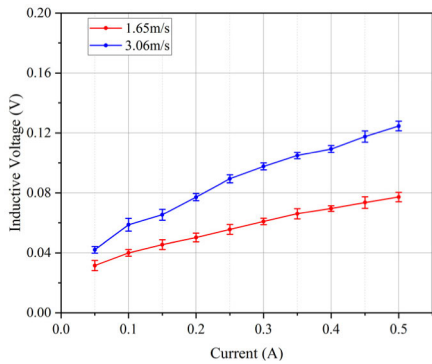
(b)

FIGURE 11. Inductive voltages at different current. (a) Middle coil. (b) Surrounding coil.
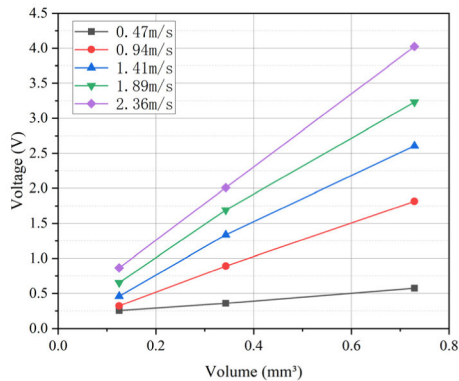

FIGURE 12. Inductive voltages with different particle volumes (0.125 mm³; 0.343 mm³; 0.729 mm³).

pipelines, the 100 mg/L lubricating oil sample was configured with ferromagnetic particles under 13 μm when the excitation current is 0.5A, and the inductive voltage signal waveform is shown in Fig. 14. The experimental particles were sieved through a 1000 mesh sieve, which ensured that the particles were smaller than 13 μm. The peristaltic pump used in the experiment was driven by a stepper motor, and the sensor flow rate reached 570 ml/min during the experiment, which was an improvement over the previous sensor.

In the single wear particle experiment, we found crosstalk between the surrounding coils and the middle coil. A dynamic oil experiment was conducted to explore whether crosstalk
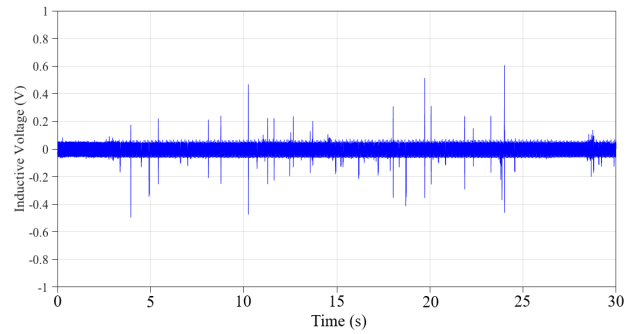
(a)
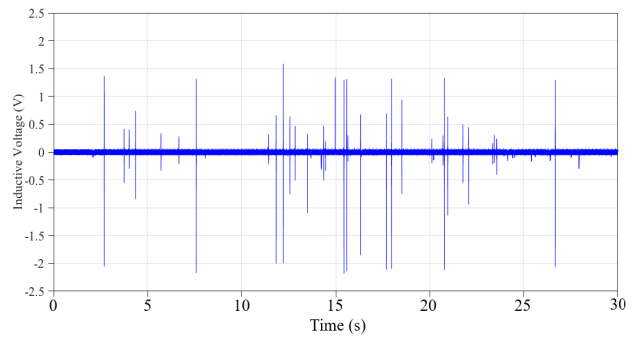
(b)

FIGURE 13. Oil sample signals with different particle concentrations (300 μm). (a) 5 mg/L; (b) 10 mg/L.

TABLE 1. The detection performance comparison of sensors.

Reference number for sensor	D_P (diameter of minimum detection particles)	D_s (equivalent inner diameter of the oil pipe)	D_p/D_s
18	75 μm	1 mm	0.075
19	20 μm	1 mm	0.02
20	50 μm	3 mm	0.0167
21	120 μm	34 mm	0.0035
22	25 μm	1.5 mm	0.0167
This paper	13 μm	5.03 mm	0.0026

influenced the particle signal. As shown in Fig. 14, since the particles in the oil were smaller than 13 μm, when the lubricating oil passed through the surrounding pipes, the middle coil signal was not affected by crosstalk. Such a result is beneficial to the detection of the sensor, which can ensure that the small wear particles are not affected by other particles in the pipeline while being detected. Based on the symmetric toroidal static magnetic field, the structures of the six surrounding coils were identical. Thus, there was only the signal from one coil and the adjacent coil, which could represent other inductive coils. The ability to detect tiny wear debris at such a large flow rate is needed for condition-based maintenance of large rotating and reciprocating machines.

E. COMPARISON WITH OTHER INDUCTIVE METHODS
Our proposed sensor based on inductive methods performed well under different toroidal magnetic field conditions.
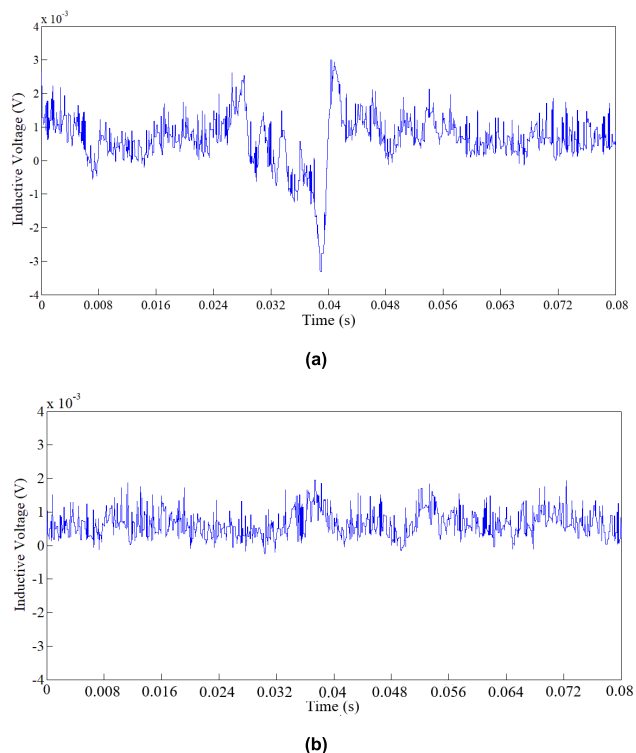
(a)

(b)

FIGURE 14. Signals of different coils under dynamic oil experiment with particles smaller than 13 μm. (a) The coil where the particles are located. (b) Another coil.

To compare this sensor with other sensors, we compared D_p (the diameter of minimum detection particles) and D_s (the equivalent diameter of the internal flow channel of the sensor) from different sensors. In this study, the equivalent diameter of the seven pipes was 7.94 mm. For intuitive comparison, we compared the ratio of D_p/D_s with some references, which is shown in Table 1. The ratio of D_p/D_s should be as small as possible to satisfy the needs for large flow and high detection accuracy. According to the data in Table 1, the ratio of our proposed sensor was 0.0026, which was the smallest among the inductive sensors in the literature [18]–[22].
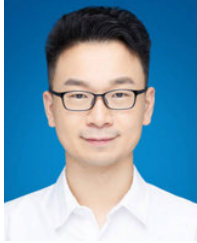
V. CONCLUSION

In this paper, a wear particle detection sensor with multiple inductive coils under a toroidal magnetic field is designed to estimate the inductive voltage of the coils caused by the wear particles. The sensor placed multiple inductive coils at the approximate strong magnetic field position, which improved detection accuracy. The experiments considered the excitation current, velocity, and volume of wear particles, and the results verified the linear relationship between the inductive voltage and the particles. We also studied the crosstalk between two adjacent inductive coils. Based on a single particle experiment and dynamic oil experiment, although there was interference between each inductive coil, the crosstalk signal was small and was masked by noise. The sensor with multiple inductive coils measured iron particles as small as 13 μm at a flow rate of 570 mL/min. More inductive coils

could be added to analyze wear particle characteristics and achieve higher throughput. Compared with previous studies, the sensor is expected to provide more detailed information about lubricants for online machine condition monitoring.

REFERENCES

[1] W. Bartelmus and R. Zimroz, "Vibration condition monitoring of planetary gearbox under varying external load," *Mech. Syst. Signal Process*, vol. 23, no. 1, pp. 157–246, Jan. 2019.

[2] C. S. Byington, M. J. Watson, J. S. Sheldon, and G. M. Swerdon, "Shaft coupling model-based prognostics enhanced by vibration diagnostics," *Insight-Non-Destructive Test. Condition Monitor.*, vol. 51, no. 8, pp. 420–425, Aug. 2009.

[3] C. K. Tan, P. Irving, and D. Mba, "A comparative experimental study on the diagnostic and prognostic capabilities of acoustics emission, vibration and spectrometric oil analysis for spur gears," *Mech. Syst. Signal Process.*, vol. 21, no. 1, pp. 208–233, Jan. 2007.

[4] B. J. Roylance, J. A. Williams, and R. Dwyer-Joyce, "Wear debris and associated wear phenomena—Fundamental research and practice," *Proc. Inst. Mech. Eng., J, J. Eng. Tribol.*, vol. 214, no. 1, pp. 79–105, Jan. 2000.

[5] B. K. N. Rao, *Handbook of Condition Monitoring*. Dordrecht, The Netherlands: Springer, 1996, pp. 35–53.

[6] R. Zimroz, W. Bartelmus, T. Barszcz, and J. Urbanek, "Diagnostics of bearings in presence of strong operating conditions non-stationarity—A procedure of load-dependent features processing with application to wind turbine bearings," *Mech. Syst. Signal Process.*, vol. 46, no. 1, pp. 16–27, May 2014.

[7] J. Edmonds, M. S. Resner, and K. Shkarlet, "Detection of precursor wear debris in lubrication systems," in *Proc. IEEE Aerosp. Conf.*, Big Sky, MT, USA, Mar. 2000, pp. 73–77.

[8] M. Kumar, P. S. Mukherjee, and N. M. Misra, "Advancement and current status of wear debris analysis for machine condition monitoring: A review," *Ind. Lubrication Tribol.*, vol. 65, no. 1, pp. 3–11, Feb. 2013.

[9] Y. Peng, T. Wu, S. Wang, and Z. Peng, "Oxidation wear monitoring based on the color extraction of on-line wear debris," *Wear*, vols. 332–333, pp. 1151–1157, May 2015.

[10] A. Hamilton, A. Cleary, and F. Quail, "Development of a novel wear detection system for wind turbine gearboxes," *IEEE Sensors J.*, vol. 14, no. 2, pp. 465–473, Feb. 2014.

[11] T. Wu, H. Wu, Y. Du, and Z. Peng, "Progress and trend of sensor technology for on-line oil monitoring," *Sci. China Technol. Sci.*, vol. 56, no. 12, pp. 2914–2926, Dec. 2013.

[12] S. Murali, X. Xia, A. V. Jagtiani, J. Carletta, and J. Zhe, "Capacitive Coulter counting: Detection of metal wear particles in lubricant using a microfluidic device," *Smart Mater. Struct.*, vol. 18, no. 3, Jan. 2009, Art. no. 037001.

[13] Y. Yu, Y. Zou, M. A. Hosani, and G. Tian, "Conductivity invariance phenomenon of eddy current NDT: Investigation, verification, and application," *IEEE Trans. Magn.*, vol. 53, no. 1, pp. 1–7, Jan. 2017.

[14] I. D. Adewale and G. Y. Tian, "Decoupling the influence of permeability and conductivity in pulsed eddy-current measurements," *IEEE Trans. Magn.*, vol. 49, no. 3, pp. 1119–1127, Mar. 2013.

[15] C. Wang, M. Fan, B. Cao, B. Ye, and W. Li, "Novel noncontact eddy current measurement of electrical conductivity," *IEEE Sensors J.*, vol. 18, no. 22, pp. 9352–9359, Nov. 2018.

[16] R. Jia, B. Ma, C. Zheng, L. Wang, X. Ba, Q. Du, and K. Wang, "Magnetic properties of ferromagnetic particles under alternating magnetic fields: Focus on particle detection sensor applications," *Sensors*, vol. 18, no. 12, p. 4144, Nov. 2018.

[17] L. Han, W. Hong, and S. Wang, "The key points of inductive wear debris sensor," in *Proc. Int. Conf. Fluid Power Mechatronics*, Beijing, China, Aug. 2011, pp. 809–815.

[18] L. Du and J. Zhe, "Parallel sensing of metallic wear debris in lubricants using undersampling data processing," *Tribol. Int.*, vol. 53, pp. 28–34, Sep. 2012.

[19] L. Du, X. Zhu, Y. Han, L. Zhao, and J. Zhe, "Improving sensitivity of an inductive pulse sensor for detection of metallic wear debris in lubricants using parallel LC resonance method," *Meas. Sci. Technol.*, vol. 24, no. 7, pp. 660–664, Jun. 2013.

[20] X. Zhu, L. Du, and J. Zhe, "A 3×3 wear debris sensor array for real time lubricant oil conditioning monitoring using synchronized sampling," *Mech. Syst. Signal Process.*, vol. 83, pp. 296–304, Jan. 2017.

[21] Y. J. Ren, W. Li, G. F. Zhao, and Z. H. Feng, "Inductive debris sensor using one energizing coil with multiple sensing coils for sensitivity improvement and high throughput," *Tribol. Int.*, vol. 128, pp. 96–103, Dec. 2018.

[22] S. Feng, L. Yang, G. Qiu, J. Luo, R. Li, and J. Mao, "An inductive debris sensor based on a high-gradient magnetic field," *IEEE Sensors J.*, vol. 19, no. 8, pp. 2879–2886, Apr. 2019.

BIN FAN received the Ph.D. degree from Xi'an Jiaotong University, China, in 2018. He is currently a Lecturer with the College of Mechanical and Electrical Engineering, Inner Mongolia Agricultural University, China. His research interests include numerical analysis of wear and real-time monitoring techniques of lube oil.

YIN BAI received the M.S. degree in control science and engineering from the Chongqing University of Posts and Telecommunications, Chongqing, China, in 2017. He is currently an Assistant with the School of Advanced Manufacturing Engineering, Chongqing University of Posts and Telecommunications. His research interest includes real-time monitoring techniques of lube oil.

PENG ZHANG is currently a researcher-level Senior Engineer with the State Key Laboratory of Smart Manufacturing for Special Vehicles and Transmission System, dedicated to design technology for special vehicles.

YONG LIU is currently a researcher-level Senior Engineer with the State Key Laboratory of Smart Manufacturing for Special Vehicles and Transmission System, dedicated to design technology for special vehicles.
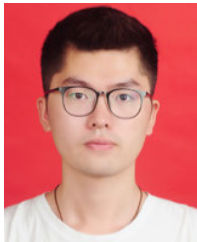
LEILEI YANG received the bachelor's degree in automation from the Southwest University of Science and Technology, China, in 2018. He is currently pursuing the master's degree in industrial engineering with the Chongqing University of Posts and Telecommunications, China. His research interest includes real-time monitoring techniques of lube oil.

SONG FENG (Member, IEEE) received the Ph.D. degree from Xi'an Jiaotong University, China, in 2016. He is currently an Associate Professor with the School of Advanced Manufacturing Engineering, Chongqing University of Posts and Telecommunications, China. His research interest includes real-time monitoring techniques of lube oil.

• • •